Carbohydrate Polymers 112 (2014) 216–224

Contents lists available at ScienceDirect

Carbohydrate Polymers

journal homepage: www.elsevier.com/locate/carbpol

# Inducing PLA/starch compatibility through butyl-etherification of waxy and high amylose starch

Obiro Cuthbert Wokadala [a,b], Naushad Mohammad Emmambux [c], Suprakas Sinha Ray [a,b,c,*]

[a] DST/CSIR National Centre for Nanostructured Materials, Council for Scientific and Industrial Research, 1-Meiring Naude Road, Brummeria, Pretoria 0001, South Africa
[b] Department of Applied Chemistry, University of Johannesburg, Doornfontein, Johannesburg 2028, South Africa
[c] Department of Food Science, University of Pretoria, Pretoria, South Africa

ARTICLE INFO

*Article history:*
Received 2 April 2014
Received in revised form 19 May 2014
Accepted 21 May 2014
Available online 7 June 2014

*Keywords:*
Polylactic acid (polylactide)
Modified starch
Compatibility
Biopolymer composites

ABSTRACT

In this study, waxy and high amylose starches were modified through butyl-etherification to facilitate compatibility with polylactide (PLA). Fourier transform infrared spectroscopy, proton nuclear magnetic resonance spectroscopy and wettability tests showed that hydrophobic butyl-etherified waxy and high amylose starches were obtained with degree of substitution values of 2.0 and 2.1, respectively. Differential scanning calorimetry, tensile testing, and scanning electron microscopy (SEM) demonstrated improved PLA/starch compatibility for both waxy and high amylose starch after butyl-etherification. The PLA/butyl-etherified waxy and high amylose starch composite films had higher tensile strength and elongation at break compared to PLA/non-butyl-etherified composite films. The morphological study using SEM showed that PLA/butyl-etherified waxy starch composites had a more homogenous microstructure compared to PLA/butyl-etherified high amylose starch composites. Thermogravimetric analysis showed that PLA/starch composite thermal stability decreased with starch butyl-etherification for both waxy and high amylose starches. This study mainly demonstrates that PLA/starch compatibility can be improved through starch butyl-etherification.



## 1. Introduction

Renewable biodegradable materials have increasingly become important due to decreasing stocks and the negative environmental effects on of fossil fuel derived materials (Mohanty, Misra, & Drzal, 2002). Polylactide (PLA) is the most widely researched renewable biodegradable material for a vast range of industrial applications (Auras, Lim, Selke, & Tsuji, 2011; Ray, 2012). PLA is linear hydrophobic polyester that is; biodegradable, synthesized controllably; inherently biocompatible; and has good mechanical properties. The most limiting short-coming to the wide application of PLA is its high price relative to other competing polymers. In order to reduce the relative expense of PLA, attempts have been made to blend PLA with starch (Avérous & Halley, 2009). Utilization of starch in polymer composites has become attractive due to its ready availability, biodegradability, renewability, ease of chemical modifications, relatively low cost compared to other commercial biodegradable materials.

Native starch consists of granules (1–100 μm) which are made up of two glucose polymers; an essentially linear amylose and a highly branched amylopectin (Tester, Karkalas, & Qi, 2004). Some starch referred to as waxy starch may contain high amylopectin (>85% w/w) while other types contain a high amount of amylose (40–80%, high amylose starches) (Copeland, Blazek, Salman, & Tang, 2009; Tester et al., 2004). Amylose is suggested to behave as a linear polymer which facilitates intra- and extra-molecular interactions while amylopectin forms less aligned structures due to a highly branched structure (Liu, Xie, Yu, Chen, & Li, 2009).

Starch granules provide a major hindrance to application of starch based composite materials since they prevent intimate interaction between starch molecules and other polymers (Chivrac, Pollet, & Avérous, 2009). Although the disruption of starch granules through production of thermoplastic starch can reduce the detrimental effect of granules, the hydrophilic nature of thermoplastic starch hinders compatibility with hydrophobic polymers such as PLA. Studies utilizing three-component PLA-compatibilizer-starch

* Corresponding author. Tel.: +27 128412388; fax: +27 128412229.
*E-mail addresses:* rsuprakas@csir.co.za, suprakas73@yahoo.com (S.S. Ray).

http://dx.doi.org/10.1016/j.carbpol.2014.05.095
0144-8617/

systems have demonstrated improvements in PLA/starch compatibility (Huneault & Li, 2007; Zhang & Sun, 2004). Some studies have focused on utilizing two-component PLA-starch systems through chemical modification of starch with maleate-group (Dubois & Narayan, 2003; Hwang et al., 2013; Raquez, Nabar, Narayan, & Dubois, 2008; Wootthikanokkhan et al., 2012), and epoxy resins (Xiong et al., 2014).

There have been no studies reported on butyl-etherification (C4) for inducing PLA/starch compatibility. In addition, no studies that have considered the potential effects of higher amylopectin and higher amylose proportions in starch on compatibility with PLA. The objective of the present study therefore, was to determine the effect of butyl-etherification of waxy and high amylose starch on PLA/starch compatibility.

## 2. Experimental

### 2.1. Materials

The PLA utilized in the present research was a commercial grade PLA 2002D® (Natureworks LLC, USA). The PLA had an average molecular weight ($M_w$) 235 kg/mol, and a D-isomer percentage of about 4%. The density of the PLA was 1.24 g/cm$^3$ while the glass transition and melting temperatures were approximately 60 °C and 153 °C, respectively. Waxy maize starch (S9679; about 100% amylopectin) and high amylose maize starch (S4180; about 70% amylose) were obtained from Sigma Aldrich (USA). Butylene oxide (1,2-epoxybutane), sodium hydroxide, sodium sulphate and other chemicals were of analytical grade and were obtained from Merck (South Africa).

### 2.2. Preparation of butyl-etherified starch and wettability test

Butyl-etherification of high and low amylose starch was done according to Bien, Wiege, and Warwel (2001) with some modifications using a Parr stirred reactor (Parr Instrument Company, USA). The molar ratio of both sodium hydroxide and sulphate to starch was 1:2 while the molar ratio of butylene oxide to starch (as glucose) was 1:7. The reaction material was heated at 140 °C with a stirring at 250 RPM for 100 min. Non-butyl-etherified waxy and high amylose starch controls were prepared without addition of the butylene oxide and precipitated with access acetone. All the samples were freeze dried to obtain the butyl-etherified and non-butyl-etherified starch material. The hydrophobic character of the prepared starch was assessed by testing the wettability in acetone/water solutions of 90% and 45% v/v. The starches (2 g) were dispersed in an acetone/water (90%) and stirred vigorously for 30 min at room temperature. The appearance of the solutions was recorded. More water was added to the dispersions/solutions to a 30% acetone/water ratio and the appearance of the resultant solutions also recorded.

### 2.3. Proton nuclear magnetic resonance spectroscopy ($^1$H-NMR) and degree of substitution (D.S)

The grafting of the hydroxybutyl-group onto the starch molecules was confirmed with $^1$H-NMR using a Varian Mercury 400 MHz NMR spectrometer (Varian Mercury, USA). The measurements were done with dimethyl sulfoxide-d6 (D-DMSO). The D-DMSO peak was used as the internal standard and the degree of molecular substitution was then determined from the ratio of the integrals of the alkyl protons and the glycosyl ring protons according to De Graaf, Lammers, Janssen, and Beenackers (1995).

### 2.4. Fourier-transform infrared (FTIR) measurements

The FTIR of the modified starches and latter, the PLA/starch composite films, was assessed using a Perkin-Elmer spectrum 100 FTIR spectrometer (Perkin-Elmer, UK) with a diamond/ZnSe crystal under universal attenuated total reflectance. The scanning was done on the films at a resolution of 4 cm$^{-1}$ with 32 scans in the range 800–4000 cm$^{-1}$. The individual curves (for each sample) were normalized to enable comparison of peaks intensities.

### 2.5. Preparation of PLA/butyl-etherified starch composite

PLA pellets were dried overnight at 80 °C. The starches (butyl-etherified and non-butyl-etherified waxy or high amylose) and PLA at different levels of addition (10, 20, 30, 40% w/w of PLA) were accurately weighed and manually mixed. The mixtures were melting blended in a HAAKE PolyLab OS Rheomix (Thermo Electron Co., USA) at 165 °C for 10 min with a rotor speed of 80 rpm. The samples were then compression moulded into thin films (about 0.5–0.8 mm thick) with a total residence time of 10 min at 165 °C using a Carver compression mould (Carver, USA).

### 2.6. Thermal analysis

Differential scanning calorimetry (DSC) was done using a DSC-Q2000 instrument (TA Instruments, USA). The samples (about 7.5 mg) were heated at a rate of 10 °C/min from −20 °C to 200 °C. They were then held at 200 °C for 5 min in order to remove the thermal history. Cooling was then done at a rate of 10 °C/min to −20 °C and heated again 10 °C/min to 200 °C. The glass transition temperature ($T_g$), crystallization temperature ($T_c$), melting temperature (peak) ($T_m$) were determined from the second heating scan of thermogram. The degree of crystallinity ($\chi t$) was determined according to Battegazzore, Alongi, and Frache (2014) using the following equation:

$$\chi t = \left(\frac{\Delta HS}{\Delta \text{Hpla}} \times \left(1 - \frac{\%\text{wt filler}}{100}\right)\right) \times 100\% \quad (1)$$

where $\chi t$ is the degree of crystallinity, $\Delta HS$ is the melting enthalpy of a given sample, %wt is the starch weight percentage in the composites and $\Delta$Hpla is the standard PLA crystal melting enthalpy of 93 J/g (Iannace & Nicolais, 1997). The experiment was performed in triplicate.

### 2.7. Thermogravimetric analysis

Thermogravimetric analysis of the PLA-Starch blends was done using a Q500 (TA Instruments, USA) thermogravimetric analyser (TGA) instrument. The samples of similar shape and size and about 13.5 ± 0.5 mg were used. The samples were heated from 20 °C at a rate of 20 °C/min up to 600 °C under nitrogen. The resultant data was analysed using TA Universal analysis software. The temperature ($T_{max}$) at which maximum rate of degradation occurs, the thermal degradation onset temperature (5% weight loss, $T_{5\%}$) and the char value (% residue at 600 °C) were determined. The samples were analysed in triplicate.

### 2.8. Mechanical/tensile properties

The tensile strength, elongation at break, and modulus of the PLA/butyl-etherified starch composite films and their respective controls were determined according to ASTM D882 using an Instron 5966 tester (Instron Engineering Corporation, USA). The prepared films were cut into test stripes of 100 mm by 10 mm. The test stripes were conditioned in a moisture equilibration chamber with saturated magnesium nitrate solution (RH 50%, 25 °C) for 1 week. Tests

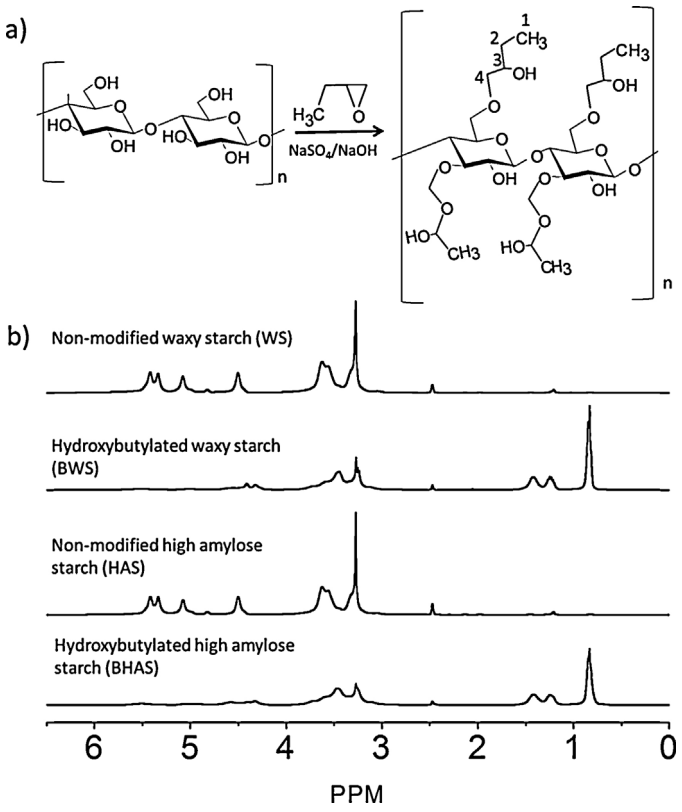


**Fig. 1.** $^{1}$H-NMR spectra of butyl-etherified and non-modified high amylose and waxy (high amylopectin) Maize Starch (a) and the associated butyl-etherification equation (b).

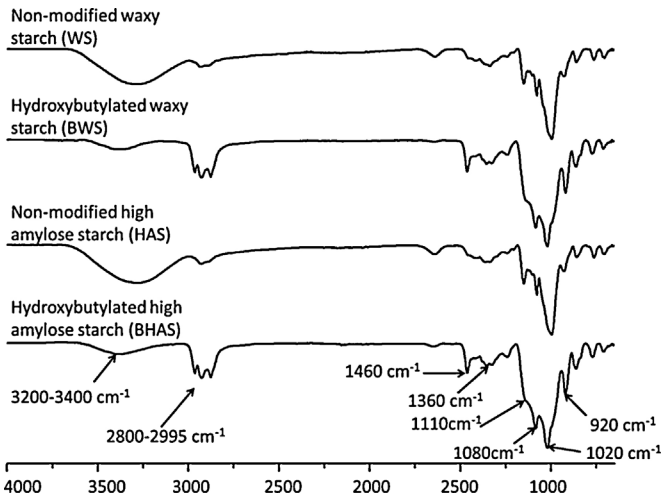


**Fig. 2.** FTIR Spectra of non-modified and butyl-etherified high amylose and waxy (high amylopectin) starch. WS = non-butyl-etherified waxy starch, BWS = butyl-etherified waxy starch, HAS = non-butyl-etherified high amylose starch, BHAS = butyl-etherified high amylose starch. The curves were normalized individually and then vertically offset for clarity.

were done immediately after equilibration and at least 10 runs were done for each treatment and the average values reported with a coefficient of variation of 10% at most.

### 2.9. Morphological characterization

The cross-sectional morphology of the PLA/starch composite films at 10% w/w and 30% w/w starch addition levels was determined using a scanning electron microscopy (SEM) (JEOL model JSM-7500F) equipment with an accelerating voltage of 5 kV. The film samples were placed in liquid nitrogen for 30 min and then freeze fractured. They were sputter coated with carbon in order to enhance conductivity. The size of distinct areas observed was determined using ImageJ software (National Institutes of Health, USA). The Ferret's diameter (longest distance along a given particle) was measured for each distinct particle and reported as an average of at least 50 particles.

## 3. Results and discussions

### 3.1. Verification of starch butyl-etherification and hydrophobic character

The equation for the butyl-etherification that was intended in this research is shown in Fig. 1a while the $^{1}$H-NMR spectra for the butyl-etherified and non-butyl-etherified waxy and high amylose starches obtained are shown in Fig. 1b. The assignment of peaks as done based on Teramoto, Motoyama, Yosomiya, and Shibata (2003). The peaks at 4.0–5.6 ppm could be assigned to the hydroxyl groups of the glucose residues. These peaks decreased when both the non-modified waxy and high amylose starch were butyl-etherified (see Fig. 1b). This indicated reduction in the glycosyl residue hydroxyl protons. Peaks corresponding to methyl/methylene protons were observed at 0.082 ppm (position 1 of Fig. 1a), 1.24 ppm (positions 2 and 4 on Fig. 1a), and 1.42 ppm PPM (position 3 on Fig. 1a) were observed for the butyl-etherified waxy and high amylose starches. These indicated the grafting of the hydroxybutyl-group to the starch residues.

The FTIR spectra of non-butyl-etherified waxy starch, butyl-etherified waxy starch, non-butyl-etherified high amylose starch and butyl-etherified high amylose starch are shown in Fig. 2. There was a strong broad peak for the non-butyl-etherified starches in the range 3200–3400 cm$^{-1}$ (Fig. 2). This peak can be attributed to stretching of glycosyl—OH groups. This peak was diminished in the both the butyl-etherified waxy and high amylose starches (Fig. 2). This indicated a decrease in the glycosyl—OH groups due to substitution by the hydroxybutyl-group. The FTIR spectra of the butyl-etherified waxy and high amylose starches also showed peaks at 2800–2995 cm$^{-1}$ due to symmetric C—H vibration in the methyl/methylene component of hydroxybutyl group added (Fig. 2). The methyl/methylene components of the hydroxybutyl group in the butyl-etherified waxy and high amylose starches also led to distinct —CH asymmetric and symmetric stretching vibrations peaks at 1460 and 1360 cm$^{-1}$. There was also an increase in the intensity of the peak at 1110 cm$^{-1}$ due C—O bond stretching which indicated of attachment of the hydroxybutyl group to the glucose residues in the starch. Similar results showing increases in decreases stretching of glycosyl—OH, incidence of new symmetric C—H vibrations and —CH asymmetric/symmetric vibrations have been reported for carboxymethylated (Yuen, Choi, Phillips, & Ma, 2009) and propyl-etherified (Teramoto et al., 2003) starches.

From the NMR and FTIR results (Figs. 1b and 2, respectively), there was apparently no clear difference in substituted starch between the waxy and high amylose starch. The calculated degrees of substitution of the butyl-etherified high amylose starch (HAS) and waxy starch (D.S) were 2.1 and 2.2, respectively. From the wettability test (Fig. 3), it could be noted that the butyl-etherified waxy starch and high amylose starches were soluble in the relatively non-polar system (90% acetone) (Fig. 3a). On changing of the system to a more polar one (30% acetone, 70% water), the modified starches precipitated (Fig. 3b). This indicated that the starch modification by butyl-etherification gave a more hydrophobic starch for both waxy and high amylose starch when compared to the respective control samples that were not modified.

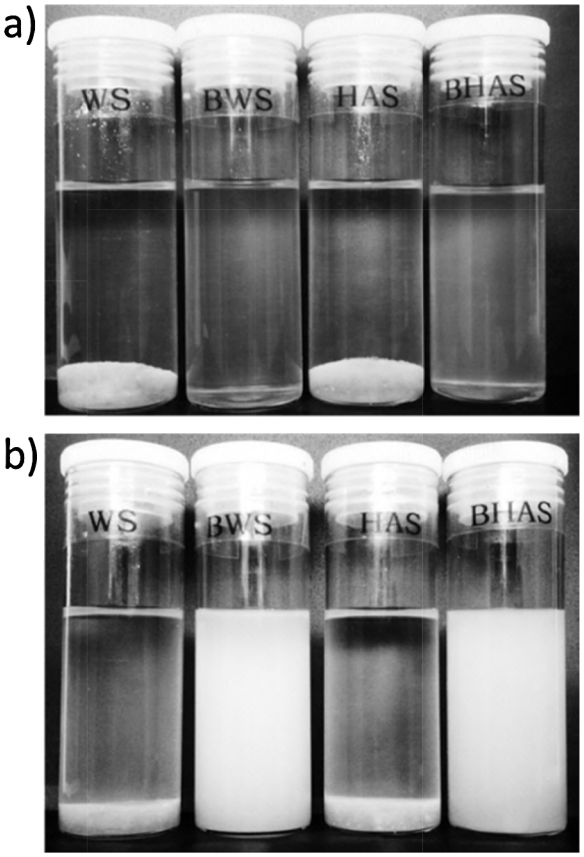


**Fig. 3.** Wettability of waxy (WS), butyl-etherified waxy (BWS), high amylose (HAS), and butyl-etherified high amylose (BHAS) starch in acetone/water solutions at 90% v/v (a) and after adding extra water to 30% v/v (acetone/water) (b). BWS = butyl-etherified waxy starch, WS = non-butyl-etherified waxy starch, BHAS = butyl-etherified high amylose starch, HAS = non-butyl-etherified high amylose starch.

### 3.2. Thermal properties

Fig. 4 shows the DSC thermograms of the PLA/hydrobutylated starch composites and the control samples (neat PLA and PLA/starch composites with non-butyl-etherified starches) for both waxy and high amylose starches. The PLA glass transition temperature ($T_g$) (60 °C) decreased with increased amounts of butyl-etherified starches while addition of the non-butyl-etherified did not affect the glass transition. The $T_g$ of PLA/starch blends containing butyl-etherified waxy starch were 58, to 54, 50 and 47 °C while that for the blends containing butyl-etherified high-amylose maize starch were 57, 50, 45 and 38 °C at 10, 20, 30 and 40% addition, respectively. Addition of the control starches (non-butyl-etherified), did not affect the $T_g$ of PLA. At the different starch addition levels, the blends containing butyl-etherified waxy starch lead to a lower reduction in $T_g$ compared to those with butyl-etherified high-amylose starch (see Fig. 4a and b). A reduction in PLA $T_g$ with addition of the butyl-etherified starches indicated that there was improved compatibility between PLA and the starches due to butyl-etherification. This was probably due to the increased hydrophobic character of the starch (as indicated by wettability test) which allowed for better distribution of the starch in the PLA matrix hence leading to a plasticizing effect. The increased hydrophobicity of the starches could have facilitated plasticizing effect of the starches PLA hence a decrease in $T_g$. Such plasticizing effects by modified starch were suggested to result from the presence of bulky added hydrophobic side chains on the starch by Aburto et al. (1997). The more bulky nature of the amylopectin molecules compared to amylose probably contributed to the greater plasticizing observed for butyl-etherified waxy starch compared to the butyl-etherified high amylose starch.

The cold crystallization peak temperature decreased with increased amounts of added butyl-etherified waxy and high-amylose starches (see Fig. 4a and b, respectively). While those containing non-butyl-etherified starches did not show any clear crystallization activity (see Fig. 4c and d). It should be noted that cold crystallization of PLA in a DSC experiment is an experimental condition generated phenomenon which depends on the cooling and heating conditions used. However, cold crystallization can be used for comparison of the crystallization between samples under the same experimental conditions. The PLA cold crystallization temperatures of the blends containing butyl-etherified waxy maize starch were 131, 126, 124 and 113 °C; those for the blends with butyl-etherified high-amylose maize starch were 128, 109, 98 and 93 °C at 10, 20, 30 and 40% starch, respectively. It could be noted that, the cold crystallization temperatures were lower with addition of butyl-etherified high-amylose starch compared to butyl-etherified waxy starch at corresponding levels of addition. Butyl-etherification of starch apparently causes nucleating effects which are greater for high amylose starch compared to high amylopectin starch. Nucleating effects of modified starches on PLA were also recently reported by Hwang et al. (2013) and Ouyang et al. (2012).

Melting endotherm consisting of two co-operative melting peaks was observed at higher addition of both butyl-etherified waxy (see Fig. 4a) and high amylose (see Fig. 4b) starch. This effect was observed at only 40% w/w addition level for PLA/butyl-etherified-waxy-starch composites while it started at 20% addition PLA/butyl-etherified-high-amylose-starch composites. Co-operative-melting peaks indicate a meta-stable crystalline structure. Therefore, at a particular corresponding starch addition level, the PLA/butyl-etherified-waxy-starch composites crystallites were probably different from those in PLA/butyl-etherified-high-amylose-starch composites. This implies that the starch amylose/amylopectin ratio possible modulates the structure of PLA crystallites in PLA/butyl-etherified starch composites.

The $T_m$ decreased with the addition of the butyl-etherified waxy and high-amylose starches (see Fig. 5a and b, respectively). The addition of non-butyl-etherified starches at the different levels of addition did not affect the PLA melting temperature (see Fig. 5a and b). The PLA melting temperature decreased with the addition of the butyl-etherified waxy and high-amylose starches (see Fig. 5a and b, respectively). Neat PLA had a melting temperature of 153 °C. The melting temperatures of the blends containing butyl-etherified waxy maize starch were 152, 149, 147, and 146 °C; while those for the blends with butyl-etherified high-amylose maize starch were 151, 150, 149 and 146 °C at 10, 20, 30 and 40% starch, respectively. A depression of the $T_m$ is an indication of compatibility for polymer blends (Aburto et al., 1997). The butyl-etherification hence improved the PLA/starch miscibility for both waxy and high amylose starch but high amylose starch was apparently more compatible with PLA.

The $\Delta H$ and $\chi t$ of the composites with butyl-etherified waxy and high amylose starches were higher than those of the composites with non-butyl-etherified starches at the different respective starch addition levels (see Fig. 4). The $\Delta Hm$ and $\chi t$ of composites with butyl-etherified high amylose starches were higher than those of the composites with butyl-etherified waxy starch at the different levels of starch addition. The $\Delta Hm$ and $\chi t$ of the PLA-starch composites containing butyl-etherified high amylose starch were 21 J/g ($\chi t$ = 26%), 24 J/g ($\chi t$ = 32%), 23 J/g ($\chi t$ = 35%), and 22 J/g ($\chi t$ = 40%) at 10, 20, 30 and 40% starch, respectively. The $\Delta Hm$ and $\chi t$ of the PLA-starch composites containing butyl-etherified waxy maize

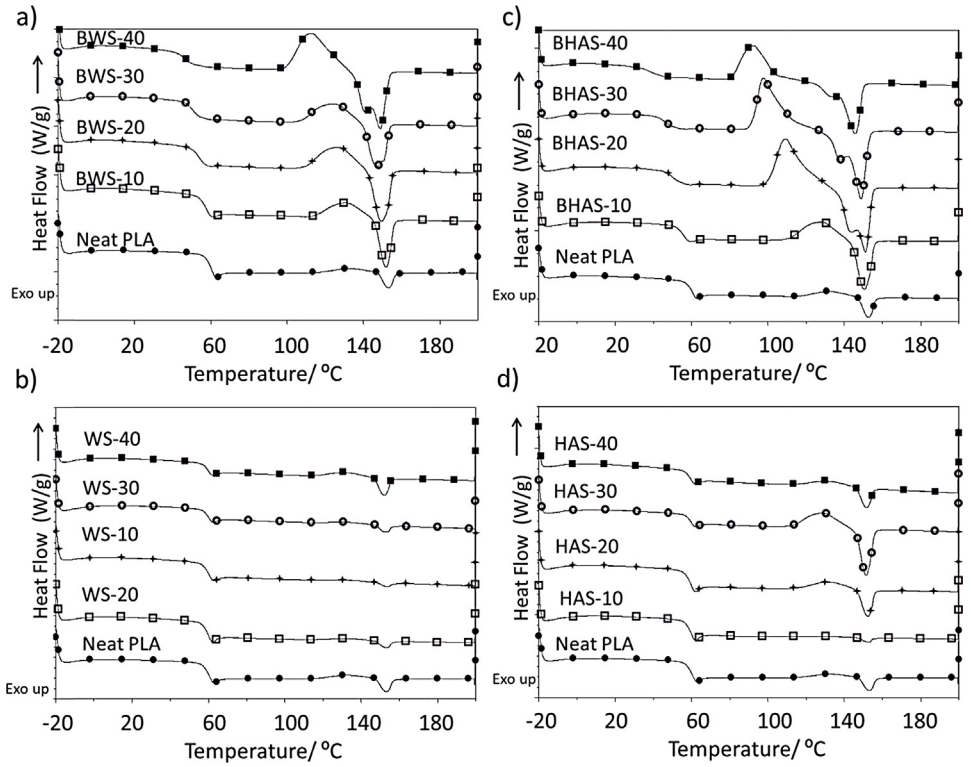


**Fig. 4.** DSC thermograms of PLA/starch composites with butyl-etherified waxy starch (a), butyl-etherified high amylose starch (b), non-modified waxy starch (c) and non-modified high amylose starch (d). BWS = butyl-etherified waxy starch, WS = non-butyl-etherified waxy starch, BHAS = butyl-etherified high amylose starch, HAS = non-butyl-etherified high amylose starch. The numbers 10, 20, 30, 40 represent the percentage (% w/w) starch addition levels and the curves presented are representative second heating scan thermograms.

starch were 9 J/g ($\chi t$ = 11%), 12 J/g ($\chi t$ = 16%), 12 J/g ($\chi t$ = 19%), and 21/g ($\chi t$ = 37%) at 10, 20, 30 and 40% starch, respectively. The $\Delta Hm$ and $\chi t$ of the PLA/starch composites with non-butyl-etherified high amylose maize starch were 1 J/g ($\chi t$ = 1%), 3 J/g ($\chi t$ = 4%), 4 J/g ($\chi t$ = 7%)and 4 J/g ($\chi t$ = 7%) while those for the composites with non-butyl-etherified waxy starch were 1 J/g ($\chi t$ = 1%), 1 J/g ($\chi t$ = 1%), 2 J/g ($\chi t$ = 2%) and 4 J/g($\chi t$ = 7%) at 10, 20, 30 and 40% starch, respectively. The higher $\Delta Hm$ and $\chi t$ values for PLA/butyl-etherified high amylose starch composites compared to PLA/butyl-etherified waxy starch composites indicated that butyl-etherified high amylose starch probably had a higher PLA nucleation effect than butyl-etherified waxy starch. The stronger nucleating effect of the butyl-etherified high amylose starch on PLA is probably due close PLA/starch interactions in PLA/butyl-etherified high amylose starch composites as a result of the essentially linear structure of amylose.

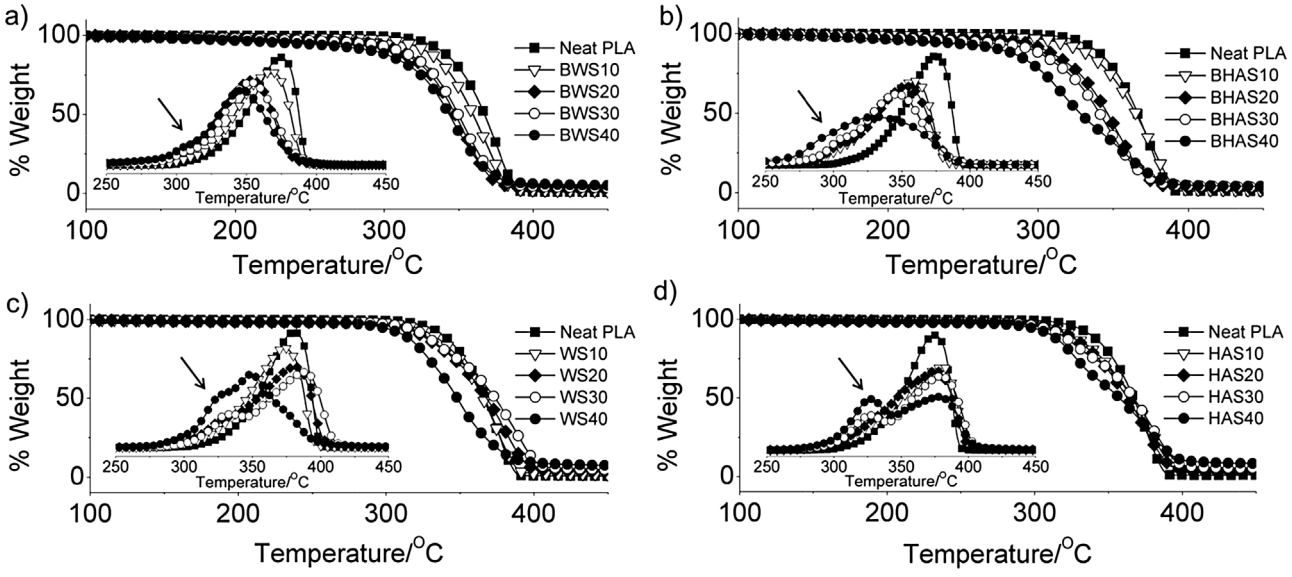


**Fig. 5.** Thermogravimetric properties of PLA/starch composites with butyl-etherified waxy starch (a), butyl-etherified high amylose starch (b), non-butyl-etherified waxy starch (c) and non-butyl-etherified high amylose starch (d) showing the weight loss (main graphs) and derived weight loss (inset graphs). PLA = polylactide; B = butyl-etherified; WS = waxy starch; HAS = high-amylose starch. The numbers 10, 20, 30, 40 represent the percentage (% w/w) starch addition levels.

**Table 1**
TGA parameters of PLA/starch composites with butyl-etherified waxy starch (BWS), butyl-etherified high amylose starch (BHAS), non-butyl-etherified waxy starch (WS), and non-butyl-etherified high amylose starch (HAS) at 10, 20, 30 and 40% w/w levels of addition.

| Sample | $T_{5\%}$ | $T_{max}$ | % Residue at 600 °C |
|---|---|---|---|
| Neat PLA | 332 ± 3a | 378 ± 2bac | 0.5 ± 0.1j |
| BWS-10 | 317 ± 2cb | 369 ± 1e | 0.5 ± 0.1ji |
| BWS-20 | 292 ± 2f | 354 ± 1f | 1.4 ± 0.2g |
| BWS-30 | 284 ± 1g | 355 ± 2f | 2.3 ± 0.1fe |
| BWS-40 | 240 ± 1i | 346 ± 1g | 3.4 ± 0.7d |
| WS-10 | 320 ± 2b | 375 ± 3dc | 0.8 ± 0.2hi |
| WS-20 | 311 ± 5cd | 381 ± 3bac | 2.1 ± 0.3fe |
| WS-30 | 308 ± 2ed | 382 ± 2a | 3.8 ± 0.2dc |
| WS-40 | 298 ± 2fgf | 350 ± 2gf | 6.1 ± 0.5a |
| BHAS-10 | 305 ± 1.e | 372 ± 4ed | 0.2 ± 0.3j |
| BHAS-20 | 283 ± 4g | 353 ± 2f | 1.3 ± 0.1hg |
| BHAS-30 | 253 ± 2h | 347 ± 2g | 2.1 ± 0.2f |
| BHAS-40 | 227 ± 3j | 317 ± 3h | 2.5 ± 0.1fe |
| HAS-10 | 307 ± 2ed | 381 ± ba | 1.4 ± 0.5g |
| HAS-20 | 308 ± 1ed | 376 ± 3bdc | 2.6 ± 0.2e |
| HAS-30 | 306 ± 3ed | 380 ± 3bac | 4.0 ± 0.1c |
| HAS-40 | 295 ± 2gf | 377 ± 1bdc | 5.3 ± 0.4b |

The numbers 10, 20, 30, 40 represent the percentage (% w/w) starch addition levels. The values with the same single letter in each column are not significantly different ($p \geq 0.05$). The values reported are averages of triplicate measurements.

### 3.3. Thermal stability

Thermogravimetric analysis measurements depend on the extent of heat induced bond cleavage in a given system due to thermal energy being greater than the bond energies. Interpretation of TGA results however should be done with caution since TGA only measures the changes in weight due to released vaporized material after the bond breakages.

The TGA and the derived TGA curves for the PLA/starch composites in the present study are shown in Fig. 5 while the associated TGA parameters are shown in Table 1. The degradation onset ($T_{5\%}$) and maximum degradation rate temperatures ($T_{max}$) of PLA were significantly ($p < 0.05$) decreased with the addition of both butyl-etherified and non- butyl-etherified waxy starch and high amylose (see Fig. 5 and Table 1). The decrease in $T_{5\%}$ and $T_{max}$ observed in the present study was in accordance with results reported by other researchers with showed starch tends to reduce the thermal stability of PLA (Acioli-Moura & Sun, 2008; Chapple, Anandjiwala, & Ray, 2013; Liu et al., 2010).

The addition of both the butyl-etherified waxy and high amylose starches significantly ($p < 0.05$) decreased the $T_{5\%}$ and $T_{max}$ at respective addition levels when compared to the control samples with non-butyl-etherified waxy and high amylose starch (see Table 1). This was a surprising result since DSC results showed that the butyl-etherified starch forms (both waxy and high amylose) were more compatible with PLA compared to the non-butyl-etherified forms (see the section on DSC). The result was probably due to differences in degradation mechanisms and/or morphology of the composites. The presence of starch in PLA/starch composites is postulated initiate the degradation of PLA at lower temperatures than the neat PLA $T_{5\%}$ and $T_{max}$ through release of polar molecules which accelerate PLA degradation (Liu et al., 2010). The initiation of PLA degradation by starch is inferred from shoulders in the derived TGA before the $T_{max}$ peaks (Liu et al., 2010; Ohkita & Lee, 2006). These shoulders could also be observed at about 290–320 °C in the present research (see black arrows in inset Fig.s 5a–d). Since the butyl-etherified starches showed greater reduction in $T_{5\%}$ and $T_{max}$ of PLA compared to the non-butyl-etherified forms, it is possible that the degradation products released from the added butyl-group further enhanced the degradation of PLA. It has been also suggested that a closer interaction between the starch and PLA could facilitate faster PLA degradation (Liu et al., 2010). A closer interaction of starch with PLA in the composites with butyl-etherified starch forms (see Section 3.5) also probably contributed to faster degradation of PLA.

The residue at 600 °C significantly ($p \leq 0.05$) increased with the addition of starch for both the modified and non-modified waxy and high amylose PLA/Starch composites (see Table 1). Similar results have been reported elsewhere (Liu et al., 2010; Ohkita & Lee, 2006). The increase in the amount of residue is proposed to result from the fact that the starch yields a relatively higher yield of charred products compared to PLA (Ohkita & Lee, 2006).

### 3.4. Tensile properties

The tensile strength, elongation at break and elastic modulus of the PLA/butyl-etherified waxy and high amylose starches composites, their respective controls, and neat PLA are shown in Fig. 6. The composites with both waxy and high amylose butyl-etherified starches had significantly ($p < 0.05$) higher tensile strength at the different starch levels compared to non-butyl-etherified starches at lower concentrations (see Fig. 6a). This effect was significantly ($p < 0.05$) more pronounced for the butyl-etherified waxy starch compared with high amylose starch (see Fig. 6a).

At the respective levels of starch addition, the PLA/starch composites with butyl-etherified starches had significantly ($p < 0.05$) higher elongation at break than the composites with non-butyl-etherified starch (see Fig. 6b). The elongation at break of the PLA/starch composites containing butyl-etherified waxy starch significantly ($p < 0.05$) increased with higher starch levels while it decreased significantly ($p < 0.05$) for the composites with butyl-etherified high amylose starch and the control (non-butyl-etherified waxy and high amylose) samples (see Fig. 6b).

The modulus of all the PLA/starch composites was significantly ($p < 0.05$) lower than that of neat PLA for all the samples (see Fig. 6c). There was a significant ($p < 0.05$) decrease in the modulus for the PLA/butyl-etherified starch complexes with both waxy and high amylose starch while the complexes with the non-modified controls increased with increased starch addition. There were no clear differences in the modulus of the PLA/starch composites containing butyl-etherified waxy starch and those containing butyl-etherified high amylose starch (see Fig. 6c). Increases in the elastic modulus with increased starch addition for the control samples was a typical filler effect that is generally observed for materials with added rigid filler materials. Although the addition of the butyl-etherified waxy and amylose high starches decreased the elastic modulus, the values of the modulus remained higher than 1000 MPa which is generally an acceptable minimum for commercial plastic products.

Butyl-etherification of both waxy and high amylose starch reduces the detrimental changes in the tensile strength and elongation at break that were associated with addition of starch to PLA. Butyl-etherified waxy starch (high amylopectin) gave higher tensile strength, elongation at break, and modulus values compared to butyl-etherified high amylose starch when added to PLA. This was apparently contrary to the DSC results which indicated the butyl-etherified high-amylose starch to be more compatible with PLA. However, the fracture dynamics of polymeric materials are mainly also controlled by micron-scale phenomena (Naushad Emmambux & Stading, 2007). Therefore, these results could probably be explained by micro-scale morphological assessments.

### 3.5. Morphology

The SEM measurements were carried out using a beam voltage of 5 kV in order to avoid the degradation of the PLA films. The morphologies of composites at 10% w/w and 30% w/w starch

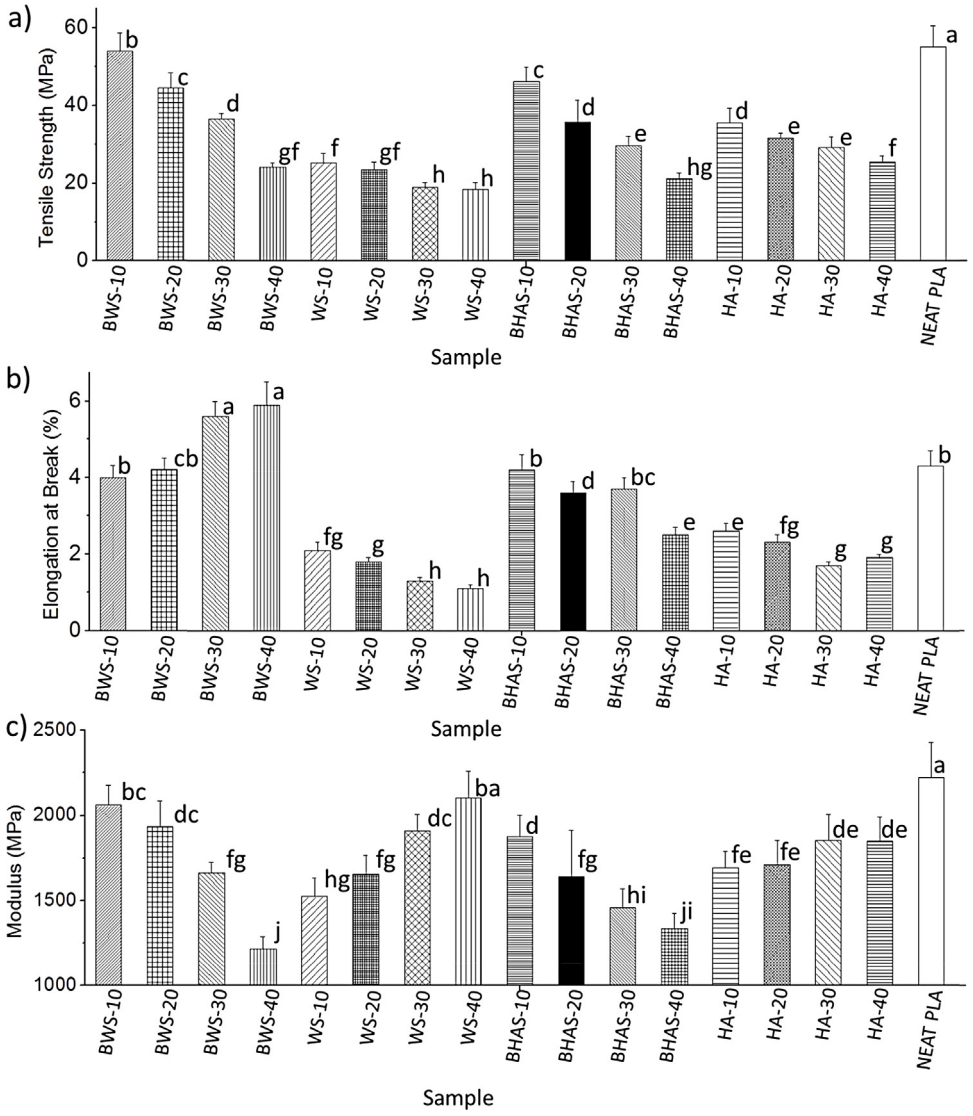


**Fig. 6.** Effect of added butyl-etherified and non-butyl-etherified high amylose and waxy starch on the tensile properties of PLA. BWS = butyl-etherified waxy starch, WS = non-butyl-etherified waxy starch, BHAS = butyl-etherified high amylose starch, HAS = non-butyl-etherified high amylose starch. The numbers 10, 20, 30, and 40 represent the percentage (w/w) starch addition level, and the columns with any single same letter are not significantly different ($p \geq 0.05$).

addition levels were presented for clarity, since they, respectively, represented composites in which tensile properties were minimally and extensively affected.

The PLA/starch composites with the butyl-etherified waxy and high amylose starches (Fig. 7a–d) seemed to have small distinct regular starch phases/particles dispersed in a continuous PLA phase. The PLA/starch composites with non-butyl-etherified waxy and high amylose starch had a rough structure with large irregular phase separated regions (Fig. 7e–h). The hydrophobic nature of the butyl-etherified starches probably reduced the PLA/starch interfacial tension in the PLA/butyl-etherified starch composites hence leading to the small distinct starch phases in the PLA/modified starch composites (Huneault & Li, 2007).

The distinct particles in composites with butyl-etherified high amylose clearly increased in size with increased starch addition (from 10% to 30% w/w, Fig. 7a and d, respectively), while in composites with butyl-etherified waxy starch increased only slightly (Fig. 7a and c, respectively). The estimated average particle diameter (ferret's distance) of the distinct regions for the PLA/butyl-etherified-high-amylose-starch composites were $1.3 \pm 0.5$, $4.9 \pm 2$ μm while that for the PLA/butyl-etherified-waxy-starch composites was $0.5 \pm 0.1$ and $0.6 \pm 0.3$ μm at 10 and 30%w/w starch addition, respectively. An apparently co-continuous phase separated structure was also observed at 30% w/w addition level for the composites with butyl-etherified waxy starch. The structure seemed to consist of a rough starch-PLA phase (dotted white arrow, Fig. 7c) and a relatively smooth PLA dominated phase (see bold white arrow, Fig. 7c).

The observed morphological differences between the composites with butyl-etherified waxy and high amylose starch could have resulted from the difference in molecular structure between amylopectin and amylose. The linear structure of amylose probably facilitated intra- and inter-molecular amylose-amylose interactions that facilitated self-aggregation of butyl-etherified high amylose starch. Amylose has a greater tendency to self-associate due to its linear structure compared to bulky and highly branched amylopectin (Putaux, Buleon, & Chanzy, 2000). This could explain the increase in size of the distinct particulate structures with increased butyl-etherified high amylose starch addition. The smaller distinct phases, and the apparent co-continuous phase

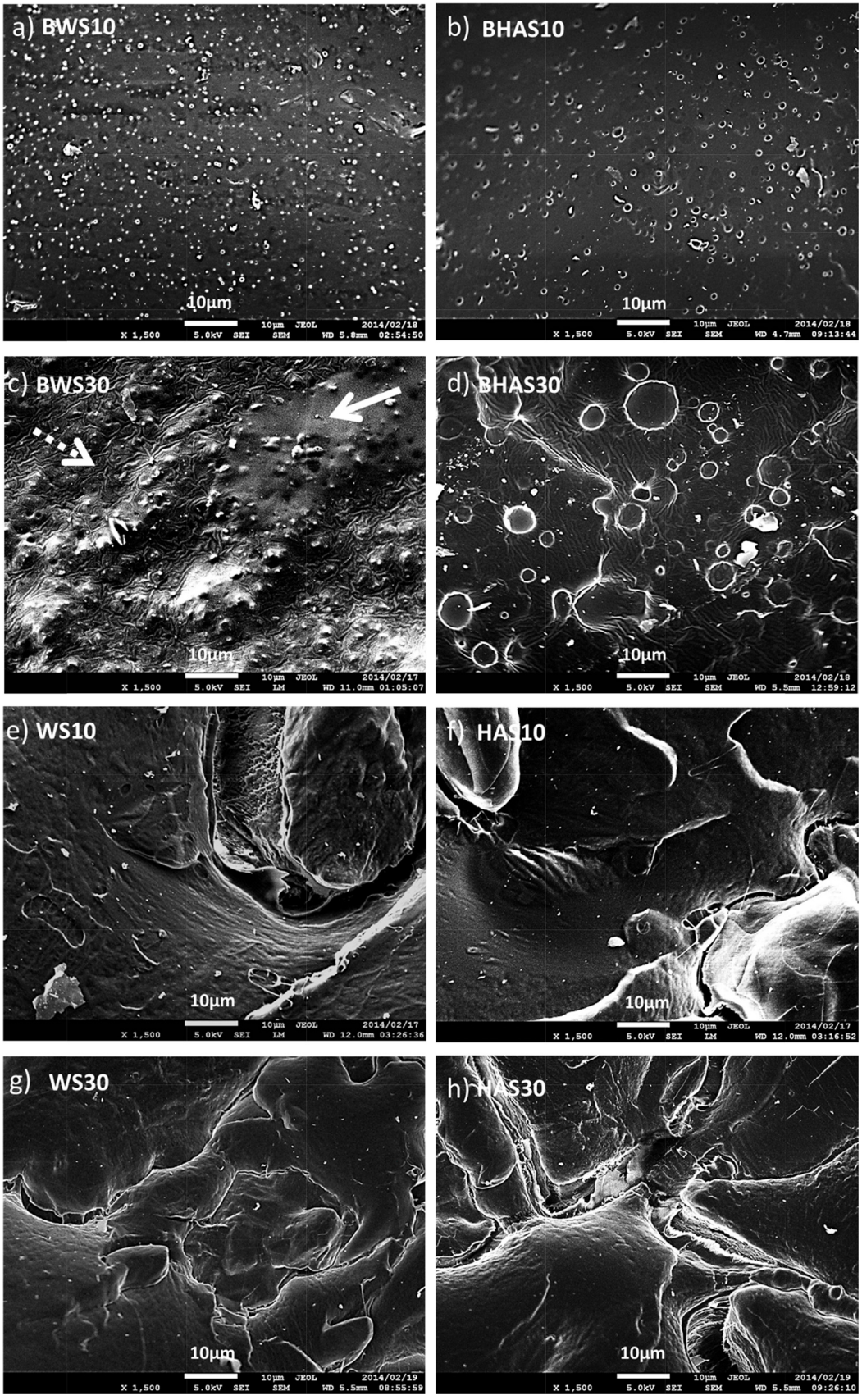


**Fig. 7.** Morphology of PLA/starch composites with added butyl-etherified waxy (BWS) and high amylose starch (BHAS), non-butyl-etherified waxy (WS) and high amylose starch (HAS) at 10% w/w and 30%w/w starch addition levels. All reported images were collected at ×1500 magnification with a 5 kV electron.

separated structure at higher starch addition level for PLA/Butyl-etherified waxy starch composites, probably favoured the transfer of tensile energy uniformly within the material compared to the larger particles of butyl-etherified high amylose starch. This probably led to higher elongation at break values observed for the PLA/starch composites with butyl-etherified waxy starch compared to those with butyl-etherified high amylose starch.

## 4. Conclusions

Butyl-etherification waxy and high amylose starch induces hydrophobicity and compatibility with PLA for both waxy and high amylose starches. Butyl-etherified high amylose starch was more compatible with PLA compared to butyl-etherified waxy starch probably due to the linear nature of the amylose which could facilitate intimate interactions between starch and PLA. The PLA/starch composites with butyl-etherified waxy and high amylose showed to improve elongation at break, tensile modulus and tensile strength compared to the composites with non-butyl-etherified starches. Morphological studies showed that butyl-etherification leads closer interaction between the starch and distinct PLA phase for both waxy and high amylose starches. At higher starch levels, composites with butyl-etherified high amylose starch give a lower elongation at break and tensile strength compared those with butyl-etherified waxy starch due to the tendency of amylose to self-aggregate. This study demonstrates that it is possible to induce PLA/starch compatibility through butyl-etherification and that the amylose/amylopectin content of the starch plays a significant role in influencing the mechanical properties of the resultant PLA/starch composites.

## Acknowledgements

O.C Wokadala and S. S. Ray thank the Department of Applied Chemistry, University of Johannesburg for the financial support. The authors also like thank the DST and CSIR South Africa for financial support.

## Appendix A. Supplementary data

Supplementary data associated with this article can be found, in the online version, at http://dx.doi.org/10.1016/j.carbpol.2014.05.095.

## References

Aburto, J., Thiebaud, S., Alric, I., Borredon, E., Bikiaris, D., Prinos, J., & Panayiotou, C. (1997). Properties of octanoated starch and its blends with polyethylene. *Carbohydrate Polymers*, *34*(1), 101–112.

Acioli-Moura, R., & Sun, X. S. (2008). Thermal degradation and physical aging of poly(lactic acid) and its blends with starch. *Polymer Engineering & Science*, *48*(4), 829–836.

Auras, R. A., Lim, L.-T., Selke, S. E., & Tsuji, H. (2011). *Poly(lactic acid): Synthesis, structures, properties, processing, and applications*. New Jersey: John Wiley & Sons.

Avérous, L., & Halley, P. J. (2009). Biocomposites based on plasticized starch. *Biofuels, Bioproducts and Biorefining*, *3*(3), 329–343.

Battegazzore, D., Alongi, J., & Frache, A. (2014). Poly(lactic acid)-based composites containing natural fillers: Thermal, mechanical and barrier properties. *Journal of Polymers and the Environment*, 1–11.

Bien, F., Wiege, B., & Warwel, S. (2001). Hydrophobic modification of starch by alkali-catalyzed addition of 1,2-epoxyalkanes. *Starch-Stärke*, *53*(11), 555–559.

Chapple, S., Anandjiwala, R., & Ray, S. S. (2013). Mechanical, thermal, and fire properties of polylactide/starch blend/clay composites. *Journal of Thermal Analysis and Calorimetry*, *113*(2), 703–712.

Chivrac, F., Pollet, E., & Avérous, L. (2009). Progress in nano-biocomposites based on polysaccharides and nanoclays. *Materials Science and Engineering: R: Reports*, *67*(1), 1–17.

Copeland, L., Blazek, J., Salman, H., & Tang, M. C. (2009). Form and functionality of starch. *Food Hydrocolloids*, *23*(6), 1527–1534.

De Graaf, R., Lammers, G., Janssen, L., & Beenackers, A. (1995). Quantitative analysis of chemically modified starches by $^{1}$H-NMR spectroscopy. *Starch-Stärke*, *47*(12), 469–475.

Dubois, P., & Narayan, R. (2003). Biodegradable compositions by reactive processing of aliphatic polyester/polysaccharide blends. In *Macromolecular Symposia* Wiley Online Library, (pp. 233–244), 198

Huneault, M. A., & Li, H. (2007). Morphology and properties of compatibilized polylactide/thermoplastic starch blends. *Polymer*, *48*(1), 270–280.

Hwang, S. W., Shim, J. K., Selke, S., Soto-Valdez, H., Rubino, M., & Auras, R. (2013). Effect of maleic-anhydride grafting on the physical and mechanical properties of poly(L-lactic acid)/starch blends. *Macromolecular Materials and Engineering*, *298*(6), 624–633.

Iannace, S., & Nicolais, L. (1997). Isothermal crystallization and chain mobility of poly(L-lactide). *Journal of Applied Polymer Science*, *64*(5), 911–919.

Liu, H., Xie, F., Yu, L., Chen, L., & Li, L. (2009). Thermal processing of starch-based polymers. *Progress in Polymer Science*, *34*(12), 1348–1368.

Liu, X., Khor, S., Petinakis, E., Yu, L., Simon, G., Dean, K., & Bateman, S. (2010). Effects of hydrophilic fillers on the thermal degradation of poly(lactic acid). *Thermochimica Acta*, *509*(1), 147–151.

Mohanty, A., Misra, M., & Drzal, L. (2002). Sustainable bio-composites from renewable resources: Opportunities and challenges in the green materials world. *Journal of Polymers and the Environment*, *10*(1-2), 19–26.

Naushad Emmambux, M., & Stading, M. (2007). In situ tensile deformation of zein films with plasticizers and filler materials. *Food Hydrocolloids*, *21*(8), 1245–1255.

Ohkita, T., & Lee, S. H. (2006). Thermal degradation and biodegradability of poly(lactic acid)/corn starch biocomposites. *Journal of Applied Polymer Science*, *100*(4), 3009–3017.

Ouyang, C., Wang, Y., Zhao, N., Liu, X., Li, S., & Zhang, Z. (2012). Preparation of poly(lactic acid) and modified starch composites. *Polymer Bulletin*, 1–11.

Putaux, J.-L., Buleon, A., & Chanzy, H. (2000). Network formation in dilute amylose and amylopectin studied by TEM. *Macromolecules*, *33*(17), 6416–6422.

Raquez, J. M., Nabar, Y., Narayan, R., & Dubois, P. (2008). In situ compatibilization of maleated thermoplastic starch/polyester melt-blends by reactive extrusion. *Polymer Engineering & Science*, *48*(9), 1747–1754.

Ray, S. S. (2012). Polylactide-based bionanocomposites: A promising class of hybrid materials. *Accounts of Chemical Research*, *45*(10), 1710–1720.

Teramoto, N., Motoyama, T., Yosomiya, R., & Shibata, M. (2003). Synthesis, thermal properties, and biodegradability of propyl-etherified starch. *European Polymer Journal*, *39*(2), 255–261.

Tester, R. F., Karkalas, J., & Qi, X. (2004). Starch—composition, fine structure and architecture. *Journal of Cereal Science*, *39*(2), 151–165.

Wootthikanokkhan, J., Wongta, N., Sombatsompop, N., Kositchaiyong, A., Wong-On, J., Isarankura na Ayutthaya, S., & Kaabbuathong, N. (2012). Effect of blending conditions on mechanical, thermal, and rheological properties of plasticized poly(lactic acid)/maleated thermoplastic starch blends. *Journal of Applied Polymer Science*, *124*(2), 1012–1019.

Xiong, Z., Ma, S., Fan, L., Tang, Z., Zhang, R., Na, H., & Zhu, J. (2014). Surface Hydrophobic modification of starch with bio-based epoxy resins to fabricate high-performance poly(lactide) composite materials. *Composites Science and Technology*, *94*(1), 16–22.

Yuen, S.-N., Choi, S.-M., Phillips, D. L., & Ma, C.-Y. (2009). Raman and FTIR spectroscopic study of carboxymethylated non-starch polysaccharides. *Food Chemistry*, *114*(3), 1091–1098.

Zhang, J.-F., & Sun, X. (2004). Mechanical properties of poly(lactic acid)/starch composites compatibilized by maleic anhydride. *Biomacromolecules*, *5*(4), 1446–1451.